Irregularities in Steady Flow for Non-Newtonian Fluids Between Cone and Plate

WERNER MICHAEL KULICKE* and ROGER S. PORTER, *Polymer Science and Engineering Department, Materials Research Laboratory, University of Massachusetts, Amherst, Massachusetts 01003*

Synopsis

Flow irregularities have been visually observed in solutions of polyacrylamide of high molecular weight on shear in a cone-and-plate rheometry (gap angle 2.3°). This anomalous flow was found to depend on molecular weight, concentration, and solvent. The onset of flow irregularities were generally at shear rates $< 5\ sec^{-1}$. A dimensional analysis shows that the elastic component of the fluid is responsible for the anomalous flow. The onset of flow irregularities has been predicted from measurements of recoverable strain as a function of shear stress.

INTRODUCTION

Flow irregularities, often described as secondary flows or flow instabilities, in cone-and-plate geometries have been observed and analyzed for Newtonian and non-Newtonian fluids by numerous investigations.[1-12] By calculating the material functions (viz., flow curves, recoverable strain, and first and second normal stress differences) for rheological properties, flow is assumed to be of a primary or laminary type. This assumption is applied to Newtonian and non-Newtonian fluids.

Walters and Waters[4] (see also reference 5) derived a theory for predicting the onset of secondary flow between a cone and plate for Newtonian fluids. Cheng[6] found reasonable agreement with this theory in tests on fluids such as *n*-hexane, water, and an aqueous 20% sucrose solution. For cone-and-plate geometries with gap angles from 1° to 4°, experimental torque values begin to deviate from predictions at a Reynolds number (Re) as low as about 800, because of the onset of secondary flow. An independent numerical solution of the equation of motion for Newtonian fluids in a cone-and-plate geometry predicts the onset of secondary flow at a higher Re of about 1200.[7] Turian has provided a fine perturbation solution for the steady Newtonian flow in cone-and-plate and parallel-plate systems.[7a]

Irregularities in non-Newtonian flow were observed by Griffiths and Walters[8] for 1.5% aqueous solution of a polyacrylamide at a gap angle of 30°. The cone and plate were surrounded by the solution. Kocherov et al.[9] found flow lines which they described as "spirals of Archimedes" for a polyethylene melt at gap angles of 10°–60°. Gleisle[10] found flow perturbations on the surface of a silicone oil. Giesekus[11] has indicated the possibility of secondary flows in rotational devices if the gap angle is smaller than 20° as a result of inertial effects. In general, for non-Newtonian fluids secondary flows have only been reported in

*On leave from Institut für Chemische Technologie, Technische Universität Braunschweig, Federal Republic of Germany.

Journal of Applied Polymer Science, Vol. 23, 953–965 (1979)

0021-8995/79/0023-0953$01.00

TABLE I
Characterization of the Polyacrylamides Used

$\overline{M}_v$, (g/mole) × 10^{-6} [a]	$[\eta]$, ml/g	$\overline{M}_w/\overline{M}_n$
1.33	335	2.5
2.53	565	2.5
4.70	930	2.5

[a] $[\eta]$ was measured in water at 25°C.

cone-and-plate geometries with gap angles above 10°, consistent with speculation.[12] Nonetheless, we have visually observed flow irregularities which seems to be vortices—in a cone-and-plate geometry at a gap angle of 2.3°. The onset of irregularities occurred at shear rates $\dot{\gamma} < 5$ sec^{-1}, as found for aqueous polyacrylamide solutions over a specific concentration and molecular weight range. The purpose of this paper is to report this unusual flow behavior, show the correspondence of flow irregularities with material functions, and to analyze the conditions for onset of the flow irregularities.

EXPERIMENTAL

The polyacrylamides

$$[CH_2\text{–}CH]_n$$
$$\quad |$$
$$H_2N\text{–}C{=}O$$

were prepared in solution with H_2O_2 as initiator in water or water plus methanol. The conversion was ≤20%. The so-called polyacrylamides were unbranched and free of initiator. Details for the polymerization have been described.[13,14] Table I describes the polyacrylamides used in this study.

Equation (1) was used to determine the molecular weight in water[15a]:

$$[\eta] = 3.67 \times 10^{-3}\, \overline{M}_v^{\,+0.81} \text{ ml/g} \tag{1}$$

This equation appears to be more appropriate for our higher molecular weights than a prior expression.[15b]

TABLE II
Inquired Aqueous Polyacrylamide Solutions in a Cone-and-Plate System at 23°C (θ = 5 cm, β = 0.04)

$\overline{M}_v$, (g/mole) × 10^{-6}	c, g/100 ml	Vortices observed	$\dot{\gamma}_{crit}$, sec^{-1}
1.33	≤5	no	—
2.53	1	no	—
2.53	2	no	—
2.53	4	yes	2.5
2.53	5	yes	2.5
2.53	6	yes	1.6
4.70	1	no	—
4.70	2	yes	4
4.70[a]	2	yes	4
4.7	5	became opaque by 0.16	

[a] Plus surfactant.

Polyacrylamide solutions with concentrations from 1% to 6% were prepared in four different solvents: water, water plus surfactant (2 wt-% dodecylsodium sulfate), ethylene glycol, and formamide. Isopropanol, 2%, was added to the water solutions to prevent viscosity changes with time.[13]

The Mechanical Spectrometer (Rheometrics Inc., Model RMS-7200) was used to determine the viscoelastic properties. The instrument allows operation in clockwise and counterclockwise directions, which is important for the determination of reliable results for small values of torque and normal force. Speed is a continuous variable from 0.001 to 250 rad/sec. Details of this instrument are given elsewhere.[16] All measurements were made at 23°C.

Flow irregularities were observed visually in cone-and-plate geometries with radii of 5 and 2.5 cm, all at a gap angle of 2.3° (0.04 rad). The 5-cm radius allowed a more precise observation for the onset of flow irregularities.

VISUAL OBSERVATIONS OF FLOW IRREGULARITIES

Flow irregularities were observed visually in steady shear at the edge of conventional cone-and-plate geometries with a 2.3° gap. Figures 1(a) to 1(e) show photos of the flow irregularities in the cone and plate for an aqueous polyacrylamide solution. At low shear rates, the visible air surface is smooth; but on in-

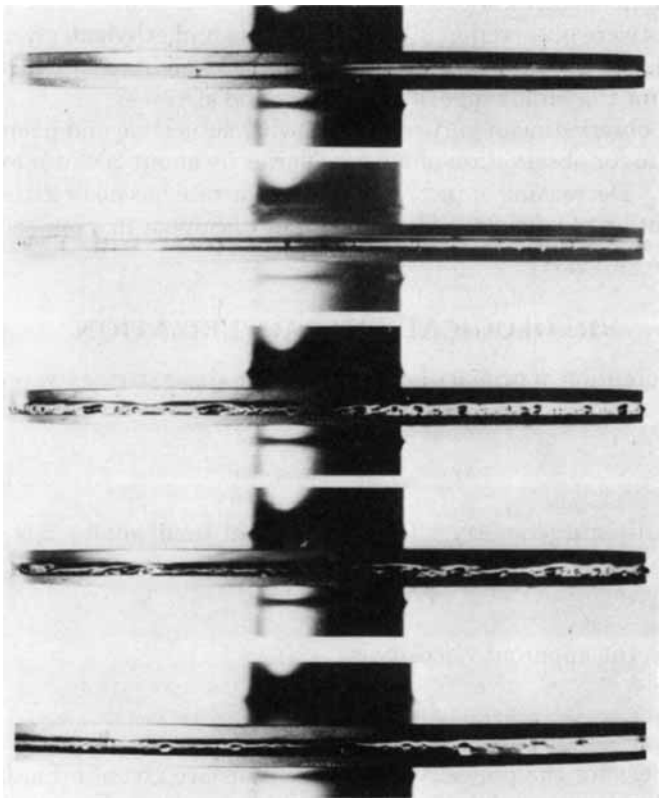

Fig. 1. Photographs of a secondary flow (vortices) in an aqueous polyacrylamide solution at four shear rates in a cone-and-plate system. The cone is at the top. $\overline{M}_v$ = 2.53 million, c = 4 wt-%, T = 23°C [θ = 5 cm, β = 0.04 rad (2.3°)]: θ is radius. (a) $\dot{\gamma}$ = 1.58 sec^{-1}; (b) $\dot{\gamma}$ = 25 sec^{-1}; (c) $\dot{\gamma}$ = 158 sec^{-1}; (d) $\dot{\gamma}$ = 625 sec^{-1}; (e) $\dot{\gamma}$ = 25 sec^{-1} [enlargement of (b)].

creasing the shear rate, flow irregularities become ever more pronounced. Figure 1(e) is an enlargement of Figure 1(b). The flow irregularities appear to be vortices. Up to 100 vortices can be observed at one time, dependent on polyacrylamide molecular weight, aqueous concentration, and shear rate. The vortices are seen to turn about their own axis at the same time they precess in the direction of shear. At a rate slower than cone rotation, the flow irregularities (vortices) are seen to jut out from the free air surface at the edge of the cone and plate. Vortex diameter is of the dimensions of the gap approaching 2 mm.

Table I lists the polyacrylamide solutions that were treated. The critical shear rate for the visually observed onset of vortices was insensitive to polyacrylamide molecular weight and concentration see (Table II). Vortices were seen up to the highest achievable shear rate, $\dot{\gamma} \approx 1000\ \text{sec}^{-1}$.

For aqueous solutions of $\overline{M}_v = 1.33 \times 10^6$, vortices were not observed at any concentration and any shear conditions. For $\overline{M}_v$ of 2.53×10^6, no vortices were seen at 2% of polyacrylamide, but vortices were observed at 4%, 5%, and 6%. Similar results were found for solutions of $\overline{M}_v = 4.70 \times 10^6$. At 5% the solution became opaque at $\dot{\gamma} \approx 0.158\ \text{sec}^{-1}$, consistent with flow irregularities. The surface was irregular, resembling melt fracture.

We also studied a solution to which a surfactant was added. We observed vortices here also, and the onset was at the same conditions as in an identical solution without surfactant.

No vortices were observed at all for formamide and ethylene glycol solvents over the same range of polyacrylamide molecular weights and concentrations (0.5%–2.0%) for the same range of shear rates and stresses.

The visual observation of vortices is somewhat subjective and irreproducible. The shear rate for observation of vortices varies by about 20%, for example, at $\dot{\gamma} = 2.5\ \text{sec}^{-1}$. Decreasing or increasing the shear rate has no or little influence on the generation of vortices. They appear or disappear in a few seconds, and the condition becomes stable.

RHEOLOGICAL CHARACTERIZATION

On the assumption of primary laminar flow, the shear stresses were calculated from eq. (2):

$$\sigma_{12} = \frac{3T}{2\pi r^3}\ \text{dynes/cm}^2 \tag{2}$$

for a cone-and-plate geometry. The shear rate at small angles, β is given by

$$\dot{\gamma} = \frac{\omega}{\beta}\ \text{sec}^{-1} \tag{3}$$

consequently, the apparent viscosity is

$$\eta = \frac{3T\beta}{2\pi r^3 \omega}\ \text{poises} \tag{4}$$

The flow curves for the polyacrylamide solutions are given in Figure 2. The arrows indicate the onset of the flow irregularities (vortices) above a critical shear rate $\dot{\gamma}_{\text{crit}}$. The vortices were visually observed at the free air surface at the edge of the circular cone and plate.

The flow curves are shown only for solutions for which flow irregularities were

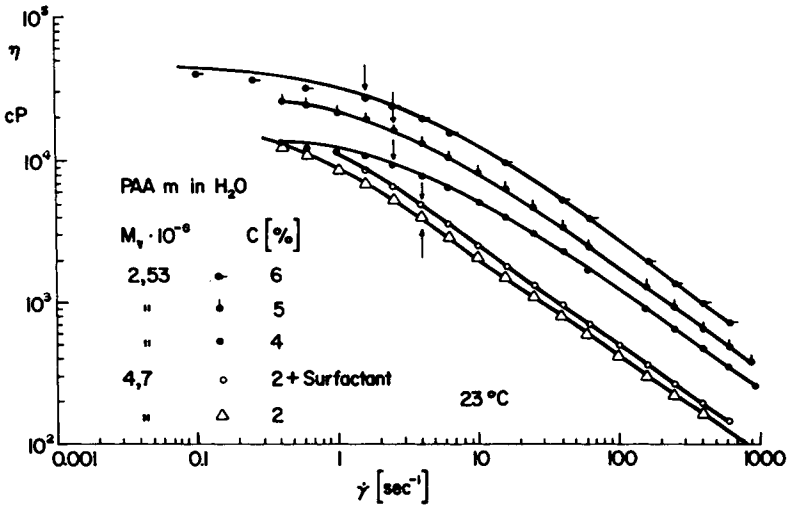

Fig. 2. Flow curves from aqueous polyacrylamide solutions for different molecular weights and concentrations. Arrows indicate minimum shear rate for observation of vortices.

observed. Note that smooth curves were obtained through the region for the onset of (vortices) flow irregularities.

Figure 3 is a plot of first normal stress difference, $\sigma_{11} - \sigma_{22}$, versus shear rate. The plots were calculated from geometry by eq. (5):

$$\sigma_{11} - \sigma_{22} = \frac{2F_z}{\pi r^2} \text{ dynes/cm}^2 \tag{5}$$

Neither average shear stress nor normal force shows a significant change in the plot for conditions where vortices were visually observed.

The time dependence of the shear stress σ_{12} and the first normal stress difference $\sigma_{11} - \sigma_{22}$ are seen in Figure 4. The onset of vortices was determined by eye at $\dot{\gamma}_{crit} \approx 2.5 \text{ sec}^{-1}$ for this solution. We see the unsteady behavior for con-

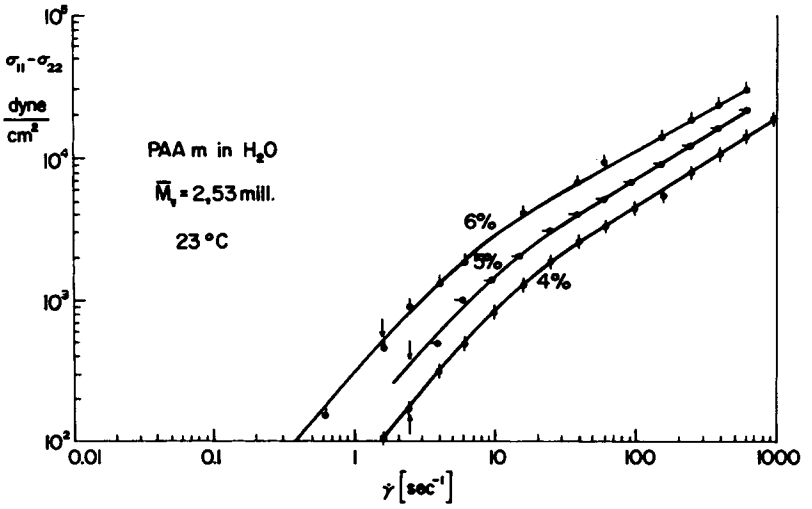

Fig. 3. First normal stress difference for aqueous polyacrylamide solutions as a function from shear rate.

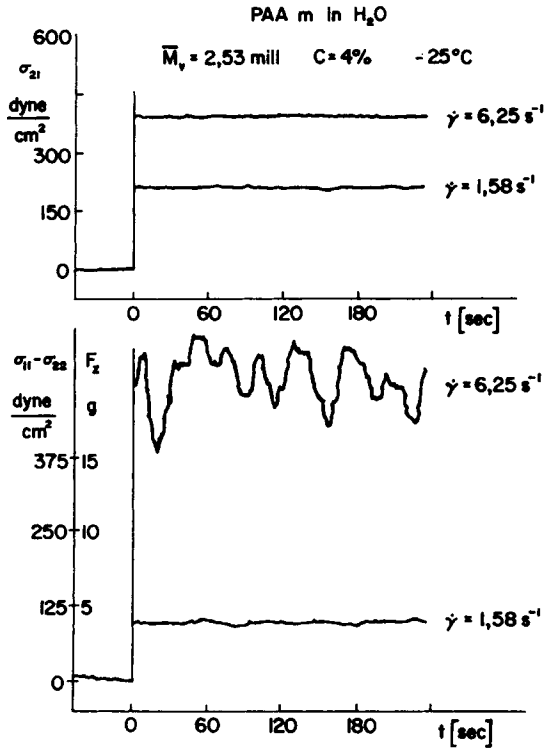

Fig. 4. Time dependence of shear stress and first normal stress difference for aqueous polyacrylamide solutions at two shear rates.

ditions of vortices only in the first normal stress. The shear stress shows no influence. For plotting the first normal stress difference versus shear rate for irregular values, an average was taken for plotting. At higher shear rates, the unsteady oscillation shear rate, the average of $\sigma_{11} - \sigma_{22}$ is independent of time and shows no marked break from the curve at lower shear rates (see Fig. 3).

DISCUSSION

Cone-and-plate rheometers are widely used to determine the viscoelastic properties of polymer systems. The common assumption is that the flow is laminar, which provides a direct solution for the equations of motion.[17] Thus, a number of precautions must be followed to ensure the existence of laminar flow between a cone and a plate. First, the gap angle should be low, generally less than about 4°.[17] The most commonly used gap angles are indeed between 1° and 4°. Adams and Lodge[18] have shown that both the error in computed shear rate and the variation of shear rate across the gap will be less than 0.5% for this case. A theoretical explanation anticipating flow irregularities (secondary flow) for angles >4° has been given.[12]

Another important and common assumption for the validity of the equation for laminar flow is that edge and inertial effects are negligible. Recently, we have shown that inertial effects, even at small gap angles, can result in a significant error in the first normal stress difference.[19] All first normal stresses in this paper are corrected for inertial effects. The maximum correction was about 150%; in one case, the nominal normal force was negative without corrections.[19]

At sufficiently small shear rates and gap angles, laminar flow is indeed normally observed for steady shear flow between cone and plate. Nonetheless, we report here the observation of flow irregularities—in the form of vortices which appear at higher shear rates and might not be seen within a conventional air thermostat where visual observations are difficult or impossible. Figure 5 shows a schematic representation for the observed flow irregularities. The addition of a surfactant has no influence on the onset conditions for irregularities nor on the nature of the vortices observed (see Fig. 2). The surfactant can expand the polymer coil.[20] This is consistent with the polymer solution plus surfactant having a higher viscosity than the same solution without surfactant.

The primary flow is laminar, and the irregularities are considered a type of secondary flow which we see as vortices. The transition from laminar to the onset of secondary flow in Newtonian fluids can be defined by the Reynolds number, *Re*:

$$Re = \frac{\text{inertial force}}{\text{viscous force}} = \frac{\rho}{\eta} D^2 \omega \beta \tag{6}$$

The *Re* represents the ratio of inertial to viscous forces and, for the special case of a cone-and-plate geometry, is represented by Eq. (6). The *Re* is defined in terms of twice the maximum gap dimension ($D \cdot \beta$) and twice the maximum linear velocity ($D \cdot \omega$). Table III shows the calculated values of *Re* using the apparent viscosity and compares these results with the theories of Walters and Waters[4,6] and of Fewell and Hellums,[7] both of which work well for Newtonian fluids. Both theories predict a transition from laminar (primary) to turbulent (secondary) flow at shear rates about 1200 sec^{-1} for Newtonian fluids calculated for our

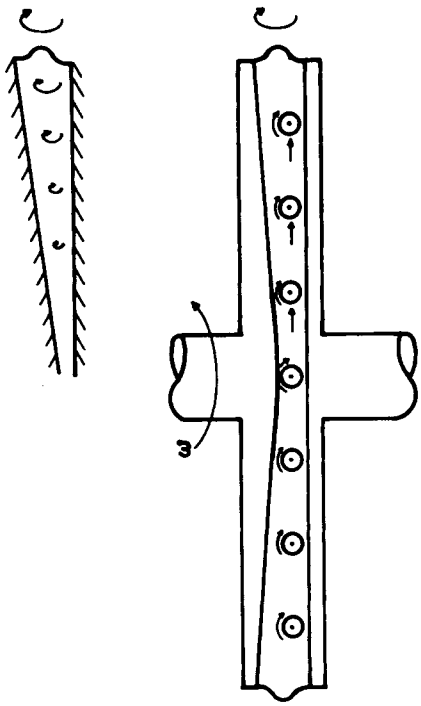

Fig. 5. Schematic representation of the visually observed vortices.

TABLE III
Calculated Reynolds Numbers[6] for Onset Conditions for Vortices and at the Maximum of the Flow Curve (See Fig. 2) for Aqueous Polyacrylamide Solutions Between a Cone and Plate (θ = 5 cm, β = 0.04)

$\overline{M}_v \times 10^{-6}$	c, wt-%	ω, rad/sec[a]	η_a, poises	Re
2.53	6	o 0.063	280	0.0009
		m 25.0	7.2	14
2.53	5	o 0.1	165	0.002
		m 3.5	3.7	38
2.53	4	o 0.1	93	0.004
		m 38.8	2.55	60
4.7	2	o 0.16	39	0.016
		m 40.0	0.92	172

[a] o = Onset conditions; m = at the maximum of the flow curve.

cone-and-plate system. These theories, however, do not predict the behavior observed for our polymer solutions. The transition region to secondary (irregular) flow for our solutions is much lower, occurring above 1–5 sec^{-1}.

The kind of flow irregularity noted here seems to be connected with elastic behavior. We thus consider a hydrodynamic theory of viscoelastic flow based on constitutive concepts which gives Cauchy's law of motion:[21,22]

$$\rho \frac{D}{Dt} V = -\nabla_p + \sum \nabla M_n + \rho f \tag{7}$$

The left term of the equation is a convective term and includes an expression of internal forces. The right side involves the pressure gradient, the viscous forces (including the deformation rate tensor) and the body forces (gravitational, magnetic, and electric fields, etc.). For a first-order fluid, using the incompressibility restriction, eq. (7) becomes

$$\rho \frac{D}{Dt} V = -\nabla_p + k_1 \nabla^2 \nabla + \rho f \tag{8}$$

These are the Navier-Stokes equations. Solution of these equations does not predict non-Newtonian viscosity nor normal stress. The only significant dimensionless group arising from these equations is the Reynolds number.

For a second-order fluid one obtains:

$$\rho \frac{D}{Dt} V = -\nabla_p + k_1 \nabla^2 V + k_2 \nabla B^2 + k_3 \nabla B_2 + \rho f \tag{9}$$

White[21,22] derived eq. (9) for a second-order viscoelastic fluid by introducing the Stokes stream function and showed by this way of dimensionless analysis that there are three significant dimensionless groups. For the special case of cone-and-plate flow one gets the following form of two dimensionless groups, eq. (10), beyond the Reynolds number of eq. (6):

$$We = \frac{\sigma_{11} - \sigma_{22}}{\sigma_{12}}$$

$$S_R = \frac{\sigma_{11} - \sigma_{22}}{2\sigma_{12}} \tag{10}$$

The Weissenberg number, We, and the recoverable shear strain, S_R, differ by a factor of 2.

The recoverable strain, S_R, is often used to predict the onset of melt fracture[20–29] as first employed by Bagley[27,28] and later by White.[21–24] Melt fracture is another type of secondary flow which differs from the irregularities observed here. A significant change in the flow curve commonly accompanies melt fracture, yet this is not the case for the elastic behavior which likely leads to the vortices observed here.

Now we would like to test whether this method is suitable to predict the onset of flow irregularities in cone-and-plate geometry. The usual way is to plot S_R versus shear stress. Figure 6 shows S_R versus shear stress for our aqueous polyacrylamide solutions which exhibited vortices. The S_R at first increases slowly with the shear stress. The first bend point corresponds well with the onset of vortices (see Table III). Then, S_R at higher shear stress increases more rapidly to a point for a second rate of change. These two bend points for rapid change correspond to two critical values of S_R and of shear stress. For polymer melts, melt fracture is also indicated by a critical S_R and shear stress.[24]

Qualitatively, we have two regions of unstable flow. In the first region vortices occur, and in the second region a gross flow disruption appears. It may be argued[23,30] that the development of vortices in the die entry region for capillary flow is also connected with a critical shear stress. At higher shear stresses it is found to be a grossly disrupted flow, i.e., melt fracture.[23] It is important to note that in polyacrylamide solutions in which no vortices were observed a critical S_R and shear stress is found (Fig. 7).

Figures 2 and 3 show the onset of visually observed vortices at low shear rates and stresses. Table IV compares values of shear rates given at the first critical point in Figure 6 and the shear rates for the onset of vortices that were visually observed. This suggests that one can determine the onset of vortices in a cone-and-plate system by plotting S_R versus σ_{12}.

The onset of a grossly disrupted flow occurs, by using the same method (S_R versus σ_{12}), at shear rates $\geq 100\ \text{sec}^{-1}$.

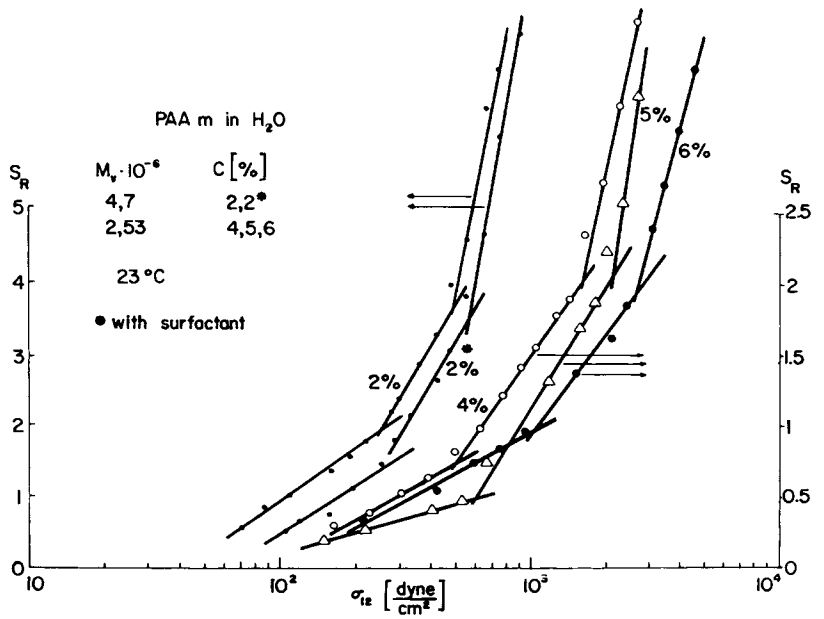

Fig. 6. Recoverable strain as a function of shear stress for aqueous polyacrylamide solutions with different $\overline{M}_v$ and several concentrations. Vortices are observed.

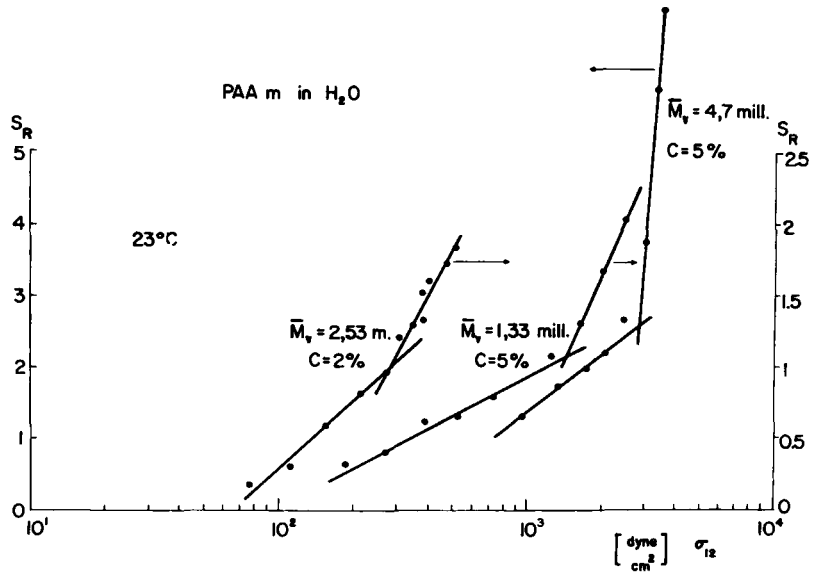

Fig. 7. Recoverable strain as function of shear stress for aqueous polyacrylamide solutions. Vortices are not observed.

For a fluid characterized by a single relaxation time, λ, for linear or nonlinear viscoelasticity, S_R is[26]:

$$S_R = \frac{1}{2} We = \lambda\dot{\gamma} \tag{11}$$

For the special case of a Maxwell model,

$$S_R = \frac{\sigma_{12}}{G} = J_e{\cdot}\sigma_{12} \tag{12}$$

because $G = \eta/\lambda$. By using Rouse's expression for equilibrium shear compliance J_e of a monodisperse polymer,[31]

$$S_R = \frac{2}{5}\frac{\bar{M}_w}{cRT}\sigma_{12} \tag{13}$$

For some polymer melts S_R is found independent of the molecular weight distribution (MWD).[32,33] It is possible that the reported insensitivity of S_R to MWD occurs only because the values of S_R were based on the difficult die swell measurement.

TABLE IV
Values of Shear Rate Calculated from the First Critical Point in Figure 6 Compared to the Values of Shear Rate—Visually Observed—at the Onset of Vortices for Aqueous Polyacrylamide Solutions

$\bar{M}_v \times 10^{-6}$	c, g/100 ml	$\dot{\gamma}$ visual onset, sec^{-1}	$\dot{\gamma}_{crit}$, S_R, sec^{-1}
2.53	6	1.5	3.5
2.53	5	2.5	5
2.53	4	2.5	9
4.7	2	4	12
4.7	2[a]	4	9

[a] Plus surfactant.

Nevertheless, for a given series of polymer samples with the same MWD in the same solvent at temperature T, one can use any molecular weight average. We will use $\overline{M}_v$, and one obtains

$$\frac{\sigma_{12} \cdot \overline{M}_v}{c} = \frac{5}{2} S_R RT = \text{constant} \tag{14}$$

Many authors have observed secondary flow for polymer fluids at the entrance of a capillary, but only a few have provided a correlation involving a dependence on molecular weight, concentration, and molecular weight distribution. In Table V we calculated these values for our polyacrylamide solutions. The σ'_{12} value is taken from the first critical point in the S_R-versus-σ_{12} diagram and indicates the onset of vortices.

Southern and Paul[30] determined a critical shear stress at the onset of entrance fracture in a capillary as a function of polymer concentration. They tested benzene solutions of polystyrene of $M_w/M_n \leq 1.2$. By using eq. (14) we can compare these results with ours (Table V).

It appears that $\sigma'_{12} \cdot (M/c)$ is a constant for a given polymer system; this means that the elastic component in the polymer fluids is necessarily responsible for this kind of secondary flow. These results also show that the nonlinear viscoelastic properties are independent of some kind of secondary flow in the form of vortices.

In summary, we have shown the existence of flow irregularities (vortices) in aqueous polyacrylamide solutions at unusually low shear rates considering the material functions $\eta = f(\dot{\gamma})$, $\sigma_{11} - \sigma_{22} = f(\dot{\gamma})$. This behavior has no noticeable influence on the plot of the material functions.

By using dimensionless analysis, it is possible to detect the onset of flow irregularities by plotting $S_R = f(\sigma_{12})$. We further suggest that there are two kinds of flow irregularities. One starts at very low shear rates $\dot{\gamma} \leqslant 5\ \text{sec}^{-1}$ where vortices become visible. Another, less visual effect starts at higher shear rates $\dot{\gamma} \geqslant 100\ \text{sec}^{-1}$. The existence of two kinds of flow irregularities is also found in capillary flow.[23,30]

TABLE V
Comparison from Polystyrene in Benzene and Aqueous Polyacrylamide Solutions Based on Eq. (14)
Vortices Observed in a Cone and Plate

Polyacrylamide $\overline{M}_v \times 10^{-6}$	$\overline{M}_w/\overline{M}_n$	c, g/100 ml	$\sigma'_{12} \cdot \overline{M}_v/c$
2.53	2.5	6	3.9×10^8
2.53	2.5	5	2.9×10^8
2.53	2.5	4	3.2×10^8
4.7	2.502	5.5×10^8	
4.7	2.5	2[a]	5.9×10^8
Flow Fracture Observed in a Capillary			
Polystyrene $\overline{M}_w \times 10^{-6}$	$\overline{M}_w/\overline{M}_n$	c, g/100 ml	$\sigma'_{12} \cdot \overline{M}_w/c$
2.0	1.2	15	2.0×10^9
2.0	1.2	17.5	2.2×10^9
2.0	1.2	20	2.0×10^9
2.0	1.2	22.5	2.2×10^9
2.0	1.2	25	1.8×10^9

[a] Plus surfactant.

Notation

η	apparent viscosity, $\eta = f(\dot{\gamma})$
$\sigma_{11} - \sigma_{22}$	first normal stress difference
σ_{12}	shear stress
$\dot{\gamma}$	shear rate
$\dot{\gamma}_{crit}$	shear rate calculated from the bend point in Figure 6
$\overline{M}_v$	viscosity-average molecular weight
$[\eta]$	intrinsic viscosity, ml/g
c	concentration, g/100 ml
β	cone angle
D	diameter
T	temperature, torque
r, ϕ	radius
ω	speed, angular velocity
F_z	normal thrust
ρ	density
B_n	kinematic tensors
M_n	$M_1 = k_1B_1$, $M_2 = k_2B_1^2 + k_3B_2$, etc., k = differential material functions
Re	Reynolds number
We	Weissenberg number
S_R	recoverable shear strain
$\dot{\gamma}_{onset,\ visually}$	shear rate at the onset of vortices visually observed
λ	relaxation time
J_e	equilibrium shear compliance
σ'_{12}	shear stress at the first bend point in Figure 6
σ''_{12}	shear stress at the second bend point in Figure 6
MWD	molecular weight distribution
$\overline{M}_w$	weight-average molecular weight
$\overline{M}_n$	number-average molecular weight

The authors express appreciation to the U.S. Army Research Office for the support of this work.

References

1. J. T. Stuart, *Ann. Rev. Fluid Mech.*, **3**, 347 (1971).
2. J. R. A. Pearson, *J. Fluid Mech.*, **4**, 163 (1976).
3. G. Astarita and M. M. Denn, in *Theoretical Rheology*, J. F. Hutton et al., Eds., 1975, p. 333.
4. K. Walters, *Rheometry*, Wiley, New York, 1975, p. 65.
5. M. J. King and N. D. Waters, *Rheol. Acta*, **9**, 164 (1970).
6. D. C. H. Cheng, *Chem. Eng. Sci.*, **23**, 895 (1975).
7. M. E. Fewell and J. D. Hellums, A.I.Ch.E. Winter Conf., Washington, D.C., Dec. 1–5, 1974.
7a. R. M. Turian, *Ind. Eng. Chem., Fundam.*, **11**, 361 (1972).
8. D. F. Griffiths and K. Walters, *J. Fluid Mech.*, **42**, 379 (1970).
9. V. L. Kocherov, Y. L. LuKach, E. A. Sporyagin, and G. V. Vinogradov, *Polym. Eng. Sci.*, **13**, 194 (1973).
10. W. Gleisle, *Rheol. Acta*, **15**, 305 (1976).
11. H. Giesekus, *Rheol. Acta*, **4**, 85 (1965).
12. A. S. Lodge, *Elastic Liquids*, Academic Press, New York, 1964.
13. W. M. Kulicke and J. Klein, *Angew. Makromol. Chem.* **69**, 189 (1978).
14. J. Klein and W. M. Kulicke, *Rheol. Acta*, **15**, 568 (1976); *Rheol. Acta*, **15**, 558 (1976).

15. (a) C. Conrad, J. Klein, and W. M. Kulicke, in preparation. (b) W. Scholtan, *Makromol. Chem.*, **14,** 169 (1954).
16. Rheometrics, Inc., *Manual for Mechanical Spectrometer*, 1974, Rheometrics, 2438 U.S. Highway #22, Union, New Jersey.
17. A. S. Lodge, *Body Tensor Fields in Continuum Mechanics*, Academic Press, New York, 1974.
18. N. Adams and A. S. Lodge, *Phil. Trans. R. Soc., Lond.*, **A256,** 149 (1964).
19. W. M. Kulicke, G. Kiss, and R. S. Porter, *Rheol. Acta*, **16,** 568 (1977).
20. S. Saito, *Kolloid-Z.Z. Polym.*, **226,** H1, 10 (1968).
21. J. L. White, *J. Appl. Polym. Sci.*, **8,** 1129 (1964).
22. J. L. White, *J. Appl. Polym. Sci.*, **8,** 2339 (1964).
23. J. L. White, *J. Appl. Polym. Sci., Appl. Polym. Symp.*, **20,** 155 (1973).
24. C. D. Han, *Rheology in Polymer Processing*, Academic Press, New York, 1976, p. 314.
25. R. Rothenberger, D. H. McCoy, and M. M. Denn, *Trans. Soc. Rheol.*, **17,** 253 (1973).
26. F. P. Smith and R. Darby, *Polym. Eng. Sci.*, **16,** 626 (1976).
27. E. B. Bagley, *J. Appl. Phys.*, **31,** 1126 (1960).
28. E. B. Bagley, *Trans. Soc. Rheol.*, **5,** 355 (1961).
29. S. Middleman, *Fundamentals of Polymer Processing*, McGraw-Hill, New York, 1977, Chap. 15.
30. J. H. Southern and D. R. Paul, *Polym. Eng. Sci.*. **14,** 560 (1974).
31. W. W. Graessley and L. Segal, *Macromolecules*, **2,** 49 (1969).
32. J. Vlachopoulos and S. Lidorikis, *Polym. Eng. Sci.*, **11,** 1 (1971).
33. J. Vlachopoulos and M. Alan, *Polym. Eng. Sci.*, **12,** 184 (1972).

Received July 25, 1977
Revised November 15, 1977